Supporting Information for:

Reduction of the Work Function of Gold by N-Heterocyclic Carbenes

Hye Kyung Kim,[†,§,‡] Alexander S. Hyla,[†,§,¶,‡] Paul Winget,[†,§,Δ] Hong Li,[†,§,¶] Chelsea M. Wyss,[†] Abraham J. Jordan,[†] Felipe A. Larrain[§,∫] Joseph P. Sadighi,[†] Canek Fuentes-Hernandez,[§,∫] Bernard Kippelen,[§,∫] Jean-Luc Brédas,[†,§,¶] Stephen Barlow,[†,§] Seth R. Marder*[,†,§]

[†]School of Chemistry and Biochemistry, Georgia Institute of Technology, Atlanta, Georgia 30332-0400, United States

[§]Center for Organic Photonics and Electronics, Georgia Institute of Technology, Atlanta, Georgia 30332-0400, United States

[¶]Solar & Photovoltaics Engineering Research Center, Division of Physical Science and Engineering, King Abdullah University of Science and Technology (KAUST), Thuwal 23955-6900, Kingdom of Saudi Arabia

[∫]School of Electrical and Computer Engineering, Georgia Institute of Technology, Atlanta, Georgia 30332-0250, United States

Contents

1. DFT-Calculated N–C–N Bond Angles for Isolated and Au-Bound NHCs

Table S1. Calculated N-C-N Bond Angles (°) for Isolated NHCs Molecules[a] and After Interacting with Au(111).

NHC	Isolated Carbene	Carbene on Gold
iPr$_2$bimy	104.2	106.4
IiPr	109.7	104.5
SIiPr	106.6	108.8
IDipp	101.4	101.5
SIDipp	105.9	105.9
6Dipp	115.5	116.1

[a]The calculations for the isolated molecules were performed with Gaussian 09[S3] at the PBE/cc-pVTZ level.

2. Method for Experimental Estimation of Coverage

XPS data (taken at normal detection angle) were corrected for photoionization cross-section and detector sensitivity. We assume that the surface N signal is not attenuated and so the intensity of the N 1s signal, corrected as described above, is directly proportional to the number of surface N atoms:

$$I_{\mathrm{N}} = k \cdot N_{\mathrm{N}} \tag{1}$$

and, therefore, that the quantity in which we are interested, N_{N}/A, the number for N atoms per unit area, is given by:

$$N_{\mathrm{N}}/\mathrm{A} = I_{\mathrm{N}}/(k \cdot A) \tag{2}$$

We also assume that the Au signal is not attenuated by the surface modifier and only by other Au atoms. We furthermore assume that the Au signal is attenuated such that:

$$I_{\mathrm{Au}}(t) = k \cdot N_{\mathrm{Au}}(t) \cdot e^{-t/\lambda_{\mathrm{Au}}} \tag{3}$$

where $I_{\mathrm{Au}}(t)/A$ is the contribution to the total Au 4f intensity from the Au atoms at depth t, $N(t)$ is the number of Au atoms at depth t and λ_{Au} is the mean free path for Au 4f photoelectrons. For Au 4f photoelectrons (for which the binding energy, BE, is ca. 86 eV) using Al Kα radiation ($h\nu$ = 1486 eV), the kinetic energy (KE), is ca. 1400 eV. The mean-free path for photoelectrons with KE > 150 eV can be estimated using the expression

$$\lambda = B(\mathrm{KE})^{0.5} \tag{4}$$

where B for Au is 0.054 nm $\mathrm{eV}^{-0.5}$,[S1] giving a value of 2.02 nm for Au 4f. Since the mean-free path is significant larger than the lattice parameter of Au ($a = b = c = 4.079$ Å; $\alpha = \beta = \gamma = 90°$) it is reasonable to treat Au has having a uniform continuous composition with the same number of Au atoms in any infinitesimal slice δt and thus to write:

$$I_{\mathrm{Au}}(t)/A = kN_{\mathrm{Au}}/V \cdot \delta t \cdot e^{-\lambda_{\mathrm{Au}}/t} \tag{5}$$

where N_{Au}/V is the number of Au atoms per unit volume, which corresponds to 4 per face-centered cubic unit cell, i.e. $4/(4.079)^3$ $\mathrm{Å}^{-3}$. The total Au intensity per unit area will be given integration of (5) from 0 (the surface) to T (the total Au film thickness); for $T >>$ ca. 3λ the value of this integral will very similar to that obtained by evaluating the integral from 0 to ∞.

$$I_{\mathrm{Au(total)}}/A = \int_0^{\infty} k \cdot N_{\mathrm{Au}}/V \cdot e^{-t/\lambda_{\mathrm{Au}}} dt \tag{6}$$

$$I_{\mathrm{Au(total)}}/A = \left[-\lambda_{\mathrm{Au}} \cdot k \cdot N_{\mathrm{Au}}/V \cdot e^{-t/\lambda_{\mathrm{Au}}}\right]_0^{\infty} \tag{7}$$

$$I_{\mathrm{Au(total)}}/A = \lambda_{\mathrm{Au}} \cdot k \cdot N_{\mathrm{Au}}/V \tag{8}$$

which, inserting values of λ_{Au} and N_{Au}/V from above gives a value of

$$I_{Au(total)}/A = k \cdot 1.19\ \text{Å}^{-2} = k \cdot (1.19{\times}10^{16}\ \text{cm}^{-2}) \quad (9)$$

Combining (2) and (9):

$$N_N/A = (I_N/I_{Au(total)}) \cdot (1.19{\times}10^{16}\ \text{cm}^{-2}) \quad (10)$$

3. Graph Showing Kelvin-Probe Work-Function Data

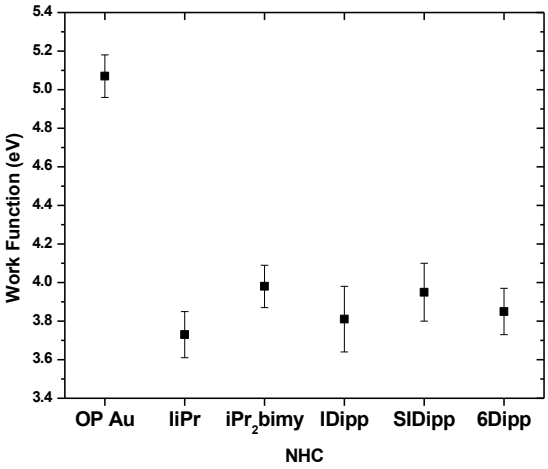

Figure S1. Work-function values measured by Kelvin Probe under nitrogen for unmodified and NHC-modified Au substrates (modified using same procedure as UPS samples, as described in the experimental section).

4. Additional XPS / UPS Data; Stability in Atmospheric and Inert Conditions

Table S2. Work-Function Values (eV) for NHC-Modified Surfaces Exposed to Ambient Conditions and Measured Using UPS.

NHC	Φ after 4 min air exposure	Φ after 24 h air exposure	$\Phi_{air} - \Phi_{init}$[a]	Φ after 7 d air exposure
none	–	–	–	5.02 ± 0.04
iPr$_2$bimy	–	3.94 ± 0.07	0.53 ± 0.17	–
IiPr	–	3.80 ± 0.13	0.51 ± 0.15	–
IDipp	–	3.94 ± 0.08	0.64 ± 0.26	–
SIDipp	4.00 ± 0.07	3.97 ± 0.02	0.45 ± 0.09	4.77 ± 0.09
6Dipp	–	3.95 ± 0.16	0.53 ± 0.30	–

[a]Difference between WF value measured before exposure to air (from Table 2) and that measured after 24 h exposure.

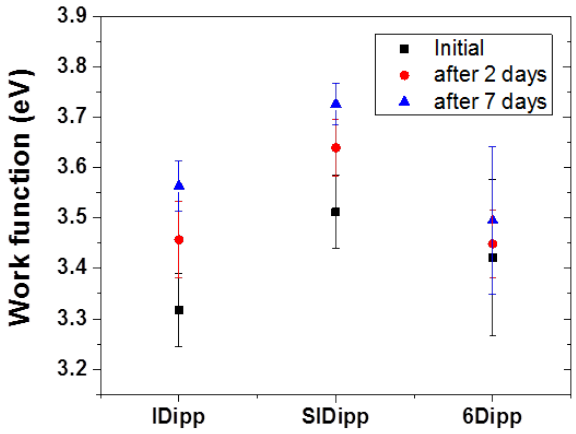

Figure S2. WF retention test (using UPS) after 2 days and 7 days of storage under nitrogen gas.

Figure S3 and S4 show XPS spectra of NHC-modified Au before and after air exposure. The urea and amide shown in Figure S5 are possible products of oxidation and hydrolysis, respectively, of **IiPr** (and are calculated using DFT to result in WF reductions of 1.00 and 0.80 eV vs. bare gold, i.e. higher WFs than **IiPr**). However, no evidence for these species is found using XPS (Figure S3) after 4 min in air: carbonyl groups are expected to show peaks at around 287.5 eV, at a higher BE than C-C groups.[S2] The O 1s spectra for before and after also shows no change to the overall peak size as shown by the good overlap of the two trials (Figure S3). Thus, the XPS is not sufficiently sensitive enable us to determine the mechanism by which the WF is raised on exposure to air. Figure 4 shows XPS spectra for **SIDipp**-modified Au before and after *7 days* air exposure; in this case there is a marked change increase in the O 1s signal (also see Table S3) and a shift in the O 1s peak to lower BE and a change in the appearance of the N 1s ionization. These data suggest clear chemical changes on air exposure, but both C 1s and O 1s spectra are clearly are again inconsistent with the presence of C=O groups (the O 1s being typically seen at BE values of ca. 533 eV).

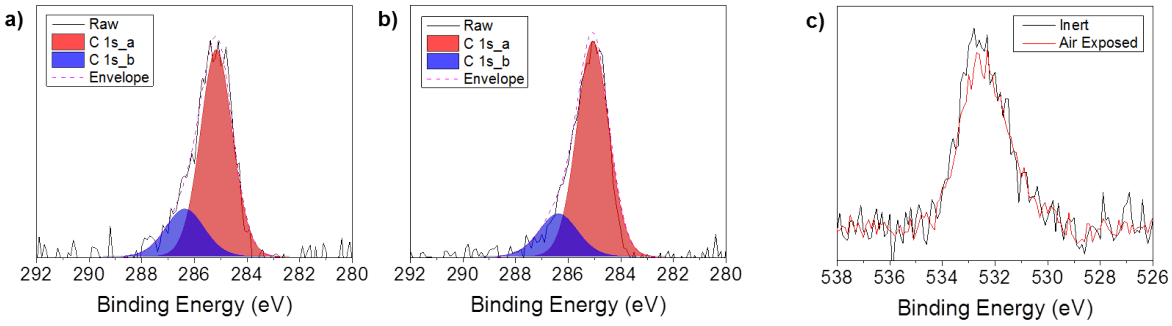

Figure S3. XPS spectra of the C 1s peak components for **IiPr** on Au a) after storage under inert conditions and b) after exposure to ambient conditions for 4 min. The spectra are very similar and were both fitted using two Gaussians (at 285.1 and 286.4 eV); no new component assignable to C=O is observed; c) O 1s peak before and after exposure to air exposure (presumably due to adventitious O-containing species), which shows a good overlap and no new components attributable to C=O or to additional surface oxide or hydroxide species.

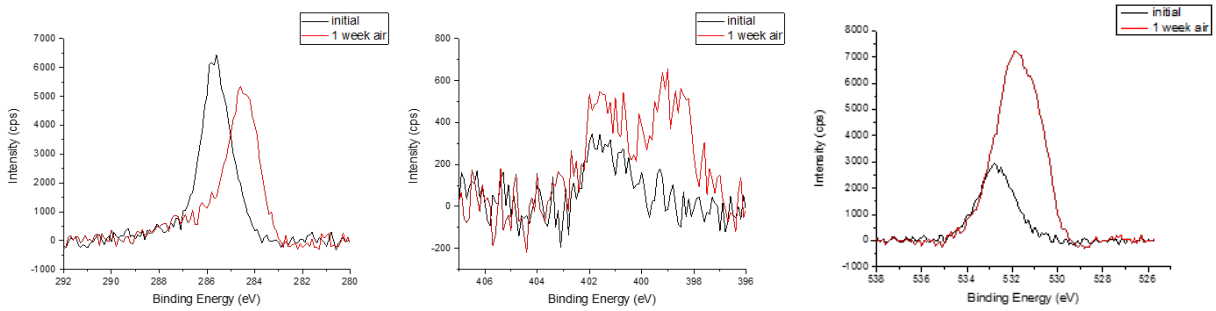

Figure S4. XPS spectra of (from left) C 1s, N 1s, and O 1s peaks for **SIDipp** on Au before and after exposure to ambient conditions for 7 days. All three ionizations shift to markedly lower BE and the O coverage increases; however, these changes are inconsistent with formation of C=O groups.

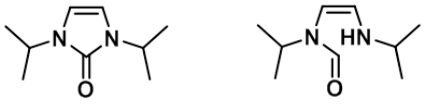

IiPr urea **IiPr amide**

Figure S5. Structures of possible NHC decomposition products of **IiPr**.

Table S3. Quantification of XPS O 1s Peaks Before and After Air Exposure for NHC-Modified Au.

NHC	O 1s / Au 4f ratio before air exposure	O 1s / Au 4f ratio after air exposure
none[a]	0.30 ± 0.04	0.36 ± 0.03
iPr_2bimy	0.30 ± 0.09	–
IiPr	0.13 ± 0.04	–
IDipp	0.20 ± 0.09	–
SIDipp	0.18 ± 0.02	0.37 ± 0.03
6Dipp	0.23 ± 0.12	–

5. Additional Plots of Geometry and Charge Redistribution

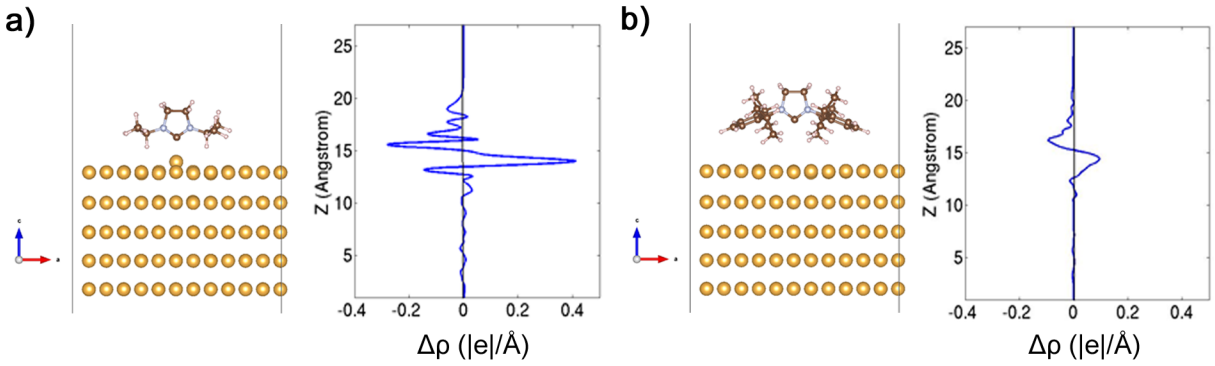

Figure S6: Optimized structure and plane-averaged change in charge density (Δρ) for (a) **SIiPr** and (b) **SIDipp** on Au.

6 Additional Plots of *J-V* Data

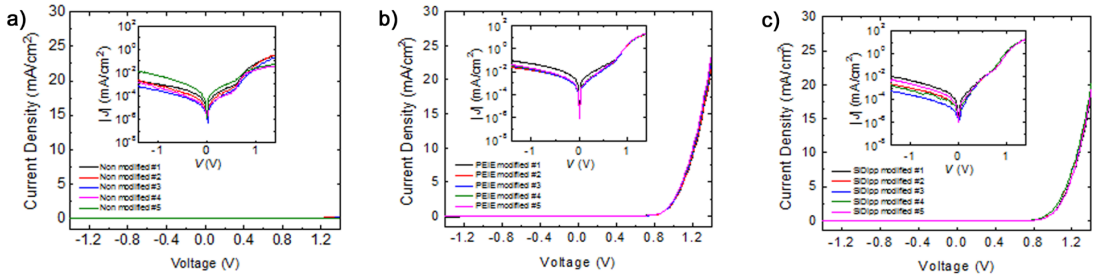

Figure S7. Semi-logarithmic plots of *J-V* characteristics showing sample-to-sample variations for devices with structure Au(with or without modification)/C_{60}(100 nm)/MoO_3(10 nm)/Ag(150 nm) using a) unmodified Au, b) PEIE-modified Au, and c) **SIDipp**-modified Au. The yield for PEIE modified devices was 93% and for SIDipp modified devices 40%.

7. References for Supporting Information

(S1) Seah, M. P.; Dench, W. A., Quantitative Electron Spectroscopy of Surfaces: A Standard Data Base for Electron Inelastic Mean Free Paths in Solids. *Surf. Interface Anal.* **1979,** *1*, 2-11.

(S2) Ago, H.; Kugler, T.; Cacialli, F.; Salaneck, W. R.; Shaffer, M. S. P.; Windle, A. H.; Friend, R. H., Work Functions and Surface Functional Groups of Multiwall Carbon Nanotubes. *J. Phys. Chem. B* **1999,** *103*, 8116-8121.

(S3) Frisch, M. J.; Trucks, G. W.; Schlegel, H. B.; Scuseria, G. E.; Robb, M. A.; Cheeseman, J. R.; Scalmani, G.; Barone, V.; Mennucci, B.; Petersson, G. A.; Nakatsuji, H.; Caricato, M.; Li, X.; Hratchian, H. P.; Izmaylov, A. F.; Bloino, J.; Zheng, G.; Sonnenberg, J. L.; Hada, M.; Ehara, M.; Toyota, K.; Fukuda, R.; Hasegawa, J.; Ishida, M.; Nakajima, T.; Honda, Y.; Kitao, O.; Nakai, H.; Vreven, T.; Montgomery, J. A., Jr.; ; Peralta, J. E.; Ogliaro, F.; Bearpark, M.; Heyd, J. J.; Brothers, E.; Kudin, K. N.; Staroverov, V. N.; Kobayashi, R.; Normand, J.; Raghavachari, K.; Rendell, A.; Burant, J. C.; Iyengar, S. S.; Tomasi, J.; Cossi, M.; Rega, N.; Millam, J. M.; Klene, M.; Knox, J. E.; Cross, J. B.; Bakken, V.; Adamo, C.; Jaramillo, J.; Gomperts, R.; Stratmann, R. E.; Yazyev, O.; Austin, A. J.; Cammi, R.; Pomelli, C.; Ochterski, J. W.; Martin, R. L.; Morokuma, K.; Zakrzewski, V. G.; Voth, G. A.; Salvador, P.; Dannenberg, J. J.; Dapprich, S.; Daniels, A. D.; Farkas, Ö.; Foresman, J. B.; Ortiz, J. V.; Cioslowski, J.; Fox, D. J. *Gaussian 09*, Gaussian, Inc.: Wallingford, CT, 2009.